International Journal for Housing Science and Its Applications
Publish September 11, 2025. Volume 47, Issue 1 Pages 921-932

https://doi.org/10.70517/ijhsa47180

Design of data acquisition and optimal scheduling algorithm for air-conditioning equipment for grid supply and demand regulation

Weishuai Wang[1], Ze Zhang[2,*], Haichao Cui[2], Jinglan Cui[2] and Chao Gao[2]
[1] State Grid Shandong Electric Power Company, Jinan, Shandong, 250001, China
[2] State Grid Dezhou Power Supply Company, Dezhou, Shandong, 253000, China
Corresponding authors: (e-mail: zhangzedq0801@163.com).

Abstract Grid supply-demand balance faces severe challenges, and air conditioning loads, as typical controllable loads, have significant demand response potential. Although the individual capacity is small, the large user base makes it a sizable demand-side resource after aggregation. In this paper, a grid supply and demand optimization scheduling method based on air-conditioning load is proposed for the grid supply and demand imbalance problem. Firstly, an indoor temperature prediction model is constructed based on the extreme learning mechanism to realize the indoor temperature prediction after 5 minutes using the historical temperature data as input, and the adjustable capacity of air conditioning load is determined accordingly. Second, an air conditioning load regulation strategy considering human comfort is designed, and the comfort temperature interval is set to 22-28°C, with the goal of minimizing the comfort cost for optimal scheduling. Finally, a supply-demand cooperative optimization model including time-of-use tariff and incentive-based demand response is constructed to optimize scheduling with the objective of minimizing the operating cost of the user's optical storage microgrid. The simulation results of the algorithm show that when the TSV index is used to evaluate the central air-conditioning load clusters, the comfort users can participate in the scheduling for 7.56 minutes, and the dispatchable capacity reaches 10.3 MW, while the economy users can participate in the scheduling for up to 21.8 minutes, and the dispatchable capacity reaches 13.8 MW. In the real-time scheduling strategy, the time granularity of 5 minutes is used during the time period 17:00-19:00 In the real-time scheduling strategy, when scheduling with 5-minute time granularity from 17:00 to 19:00, the power difference of the contact line is 0.40kW, and the number of iterations is 170, which is a significant improvement compared to the scheduling effect of 15-minute time granularity. The method in this paper provides a feasible technical path for grid supply and demand regulation.

Index Terms air-conditioning load, supply and demand regulation, extreme learning machine, temperature prediction, comfort evaluation, optimal scheduling algorithm

I. Introduction

Air conditioning equipment is one of the indispensable and important equipments in modern life, which can effectively improve indoor air quality, regulate indoor temperature, and bring people a comfortable living environment [1], [2]. However, in order to ensure the normal operation and performance optimization of air conditioning equipment, we need to collect and analyze its operation data [3].

In order to collect the operation data of air conditioning equipment, sensors need to be installed at key locations [4]. Sensors can be used to measure parameters such as temperature, humidity, air pressure, and current to obtain the operating status and environmental conditions of the equipment [5], [6]. For example, installing temperature and humidity sensors at the air inlet and outlet of air conditioning equipment can monitor the temperature and humidity changes of indoor and outdoor air in real time. Installing current sensors on the circuit board can understand the power consumption of the equipment [7]. And in order to realize the real-time and accurate collection of sensor data, a data acquisition system needs to be configured [8]. The system can connect the sensor and the computer through wired or wireless means, and transmit the data acquired by the sensor to the computer for subsequent analysis and processing [9], [10]. The data acquisition system not only needs to have high-precision and high-sensitivity acquisition capability, but also stable communication performance to ensure the reliability of data transmission [11], [12]. The design and optimization of air conditioning energy-saving system is an integral part of modern air conditioning use by collecting data and analyzing it to find out the problems of air conditioning equipment so as to optimize its design [13]-[15]. The application of energy-saving technology should be considered in the design, and corresponding measures should be taken to reduce energy consumption and improve the efficiency of the

equipment in use, only in this way can we enjoy the comfort and also minimize the pollution and pressure on the environment [16]-[19].

The stable operation of the power system requires the power balance between the supply side and the demand side, but the modern power system is faced with the severe challenge of power supply and demand imbalance. On the one hand, the proportion of renewable energy generation is increasing, and its intermittency and volatility have brought great challenges to the stability of the power grid; on the other hand, the power consumption load is characterized by high peak-valley difference and continuous growth of peak load, which leads to an increase in the pressure of power grid peaking. Traditional peaking means mainly rely on supply-side regulation, but this approach faces problems such as limited regulation capacity, slow response speed and high cost. In recent years, demand-side management has received widespread attention as a cost-effective means of balancing supply and demand. Among the various types of controllable loads, air conditioning loads have become an important resource for demand-side response due to their significant temporal and spatial distribution characteristics and large adjustable potential. Currently, air-conditioning loads participate in grid supply and demand regulation mainly face two key issues: first, how to accurately predict and assess the adjustable capacity of air-conditioning loads; second, how to achieve optimal scheduling of air-conditioning loads under the premise of ensuring the comfort of users. It is difficult for the power grid to directly dispatch massive and decentralized air-conditioning load resources, and it is necessary to establish a reasonable scheduling strategy framework and algorithms. At the same time, the regulation of air conditioning load will directly affect the user's indoor temperature environment, how to achieve a balance between load regulation and user comfort is also an important issue. In addition, different types of users have different levels of price sensitivity and different requirements for the room temperature environment, which requires the design of differentiated regulation strategies for different user characteristics. Effective air conditioning load regulation can not only improve the supply and demand balance of the grid, but also bring economic benefits to users, while reducing the peak load and operating costs of the system.

Based on the above analysis, this paper proposes a data acquisition and optimal scheduling algorithm for air conditioning equipment oriented to grid supply and demand regulation. First, an indoor temperature prediction model is established based on the historical temperature data collected by the in-home energy management device combined with an extreme learning machine, which is used to evaluate the adjustable capacity of the air conditioning load. Second, the air conditioning load regulation strategy is designed to optimize scheduling with the goal of minimizing the comfort cost, considering the comfort demand of users. Then, a supply-demand cooperative optimization model including time-of-use tariffs and incentive-based demand response is constructed to optimize the dispatch with the objective of minimizing the operating cost of the user's optical storage microgrid. Finally, the effectiveness of the proposed method is verified by arithmetic simulation.

II. Grid Supply and Demand Regulation Strategies for Air Conditioning Loads

Air-conditioning load is one of the most controllable loads with demand response potential in electric power terminal equipment. Although the individual capacity of air-conditioning load is not large, due to its large user base, if a large number of dispersed air-conditioning loads are aggregated, it will be a very considerable demand-side resource. Air-conditioning loads can be used as system backup resources and participate in the optimal dispatch of the power grid through demand-side response. However, due to the huge scheduling workload, it is difficult for the power grid to directly dispatch the huge amount of decentralized air-conditioning load resources.

II. A.Supply and Demand Regulation Strategy Framework

The process of user participation in demand-side response can be divided into three stages: pre-budgeting decision, contract signing, and response. In this paper, the strategy is built on the response implementation process after signing the contract, and the steps of its interaction strategy include.

(1) The household energy management device calculates the adjustable capacity of all air conditioners controlled by the device.

(2) The user reports its adjustable capacity to the grid control center through the energy management device.

(3) The control center comprehensively analyzes the reported capacities of all contracted users with energy management devices and issues load-shedding instructions, i.e., the total capacity for load-shedding is given.

(4) Contract users are assigned a proportional amount of load cutting in accordance with the reported capacity.

(5) Each energy management device makes its own internal designation based on the load-cutting instructions assigned to it, and issues control instructions to each air conditioner.

II. B.Adjustable capacity for air-conditioning load

The actual air conditioning operation of the indoor environment, relative humidity and air flow rate changes are relatively small, air temperature changes mainly affect the human comfort. In this paper, the comfort temperature range is set to 22~28℃. Through the historical temperature data, the establishment of a temperature prediction model to predict the future temperature of the room, so as to determine the maximum adjustable capacity in the case of ensuring the basic comfort of the room.

II. B. 1) Indoor temperature prediction

In this paper, temperature prediction is performed based on historical temperature data collected by in-home energy management devices, combined with an extreme learning machine. The extreme learning machine described in this paper is a machine learning system constructed based on feed-forward neural network (FNN), which is widely used in the field of regression problems and data prediction. In this paper, the extreme learning machine is used, and the historical temperature change data are used as input to train the extreme learning machine. The extreme learning machine method in this paper is realized by Matlab's own ELM toolbox.

The main steps of temperature prediction are as follows.

(1) Divide the day into five periods, which are 0:00~6:00, 6:00~11:00, 11:00~14:00, 14:00~18:30, and 18:30~24:00.

(2) Recalling historical temperature data from a historical database collected by the in-home energy management device at a time interval of one data point every 5s.

(3) Divide the historical temperature data into 5 parts according to the 5 times intervals described in step (1), and train each part using an extreme learning machine. Wherein, the training steps are as follows.

1) Identify and intercept temperature change data from each respective time period for the temperature rise time period. The temperature rise time period indicates that the temperature is in the shutdown or standby state at this time period, and no cooling output is made. N_0 data intervals can be obtained by this step.

2) If the interval time length of the data interval intercepted in step 1) does not exceed 5 min, this data interval is excluded, otherwise, a data pair is formed between the temperature data at a certain moment and its temperature data after 5 min, i.e., the m st temperature data and the $m+60$ nd temperature data of the data interval. In this case, the m rd temperature data is the input data and the $m+60$ th temperature data is the output data, resulting in N_i data pairs, $i=1,2,3,4,5$, representing the 5 periods of the day.

3) The extreme learning machine M_i is used to train the N_i data pairs.

II. B. 2) Calculation of adjustable capacity

The temperature data of a room at the current moment as input to the limit learning machine corresponding to each time period, the output is the temperature prediction value of the air conditioning shutdown operation for 5 min after the air conditioning shutdown operation, if the temperature of the room in the air-conditioning shutdown situation 5 min after the temperature does not exceed the comfort requirements of the temperature, this paper is set to 28 ℃, the air-conditioning equipment of the room will be labeled as adjustable, otherwise, it is labeled as non-adjustable.

Temperature prediction of all rooms with air conditioning under the in-home energy management device and labeling of all air conditioning equipment under the energy management device to obtain the adjustable capacity Q of all air conditioning loads managed by a particular in-home energy management device, calculated as:

$$Q_{\Sigma}=\sum_{i=}^{N}P_{i,r}\times u_i \tag{1}$$

In the formula: $P_{i,r}$ represents the rated power value of air conditioner i under the energy management device. u_i is the adjustable mark for the i-th air conditioner. If this air conditioner is adjustable during the control stage, then u_i =1.

II. C.Air conditioning regulation strategy

According to the analysis above, the temperature prediction is made every 5 minutes, and the corresponding air conditioner adjustable mark is also made every 5 minutes. Therefore, the air-conditioning command is also set to be issued once every 5 min, i.e., the air-conditioning status under the energy management device is updated once every 5 min, and the air-conditioning is controlled to perform the corresponding action. However, the load-shedding instruction from the power grid dispatch center is issued once every 15 min, i.e., the air-conditioner is regulated three times within the time interval of an instruction from the power grid, so it is necessary to formulate an appropriate air-conditioner control response strategy. According to the above analysis, each household energy

management device will report the adjustable capacity three times in 15 min, and the grid side selects the smallest of the three reported capacities as the adjustable capacity reference quantity of this user in the scheduling section. Based on the adjustable capacity reference quantity of the customer in the dispatching section, the grid side will issue a load-shedding instruction in conjunction with the current grid operation. The load-shedding instruction is based on the capacity reported by the household energy management device, and the load-shedding capacity is allocated proportionally and sent to each household energy management system through the grid terminal.

Each in-home energy management system develops its own air-conditioning control strategy for the air-conditioners that are in the adjustable state during the control period. Herein, this paper defines the cumulative deviation of the indoor temperature from the optimal comfort temperature brought about by the regulation command at each air conditioner regulation moment during the 15 min grid regulation period as the comfort cost CL. The objective of formulating the strategy is to minimize the comfort cost CL of the air conditioners regulated by the in-home energy management devices during the 15 min regulation period, and to set the optimal comfort temperature at 24°C and below, as follows:

$$C_L = \sum_{i=1}^{N}\sum_{j=1}^{3} C_{Lij} = \sum_{i=1}^{N}\sum_{j=1}^{3} \Delta T_{ij} j \tag{2}$$

where, ΔT_{ij} is the difference between the temperature of the i nd air-conditioner in 15 min, after the j rd period of shutdown, and the optimal comfort temperature of 24°C.

III. Optimal grid supply and demand scheduling algorithm based on air-conditioning loads

III. A. Supply and Demand Response Modeling

III. A. 1) Time-of-day tariff modeling

Based on the analysis of the characteristics of the supply and demand sides of the unit built in this paper and the discussion of the user's power consumption habits, a suitable time-sharing tariff strategy is formulated, dividing the 24 hours of a day into three time periods: peak, flat and valley, with a suitable tariff for each time period, with the aim that the user can change or adjust the load output according to the time-sharing tariff to optimize the load curve, thus improving the microgrid economic model [20].

Here they are referred to as the rate of change of customer load and the rate of change of electricity price, respectively, where the expression for the relationship between the two is:

$$\lambda_{\Delta P_{t'}} = e_{tt}\lambda_{\Delta c_t} + e_{tt'}\lambda_{\Delta c_{t'}} \tag{3}$$

where, $\lambda_{\Delta P_{t'}}$ - the rate of change of load at t moments, $\lambda_{\Delta c_t}$ -- Rate of change of electricity price at moment t, $\lambda_{\Delta c_{t'}}$ -- Rate of change of electricity price at t' moment, e_{tt} -- Auto-elasticity coefficient, $e_{tt'}$ -- Cross elasticity coefficient.

In the load curve peak, flat and valley time, after the implementation of time-sharing tariff, the user by adjusting their own electricity consumption, after the implementation of time-sharing tariff user load peak and flat and valley section of the amount of electricity is:

$$\begin{cases} Q_{f'} = Q_f - \Delta Q_f \\ Q_{p'} = Q_p - \Delta Q_p \\ Q_{g'} = Q_g - \Delta Q_g \end{cases} \tag{4}$$

where Q_f, Q_p, Q_g - electricity consumption in each period before the introduction of time-of-day tariff.

$Q_{f'}$, $Q_{p'}$, $Q_{g'}$ - the amount of electricity consumed in each period after the introduction of time-of-day tariffs.

ΔQ_f, ΔQ_p, ΔQ_g - the change in electricity consumption in each time period before and after the implementation of time-of-use tariffs.

In a time period, the current electricity consumption of the user will be affected by the electricity price of the three time periods of peak and valley leveling, according to the formula of the price elasticity coefficient of demand and the formula of the cross-price elasticity coefficient of demand, we get the formula of the price elasticity coefficient of electricity as:

$$\begin{cases} \varepsilon_{ff}=\dfrac{\Delta Q_f}{Q_f}\cdot\dfrac{p_f}{\Delta p_f} & \varepsilon_{fp}=\dfrac{\Delta Q_f}{Q_f}\cdot\dfrac{p_p}{\Delta p_p} & \varepsilon_{fg}=\dfrac{\Delta Q_f}{Q_f}\cdot\dfrac{p_g}{\Delta p_g} \\ \varepsilon_{pf}=\dfrac{\Delta Q_p}{Q_p}\cdot\dfrac{p_f}{\Delta p_f} & \varepsilon_{pp}=\dfrac{\Delta Q_p}{Q_p}\cdot\dfrac{p_p}{\Delta p_p} & \varepsilon_{pg}=\dfrac{\Delta Q_p}{Q_p}\cdot\dfrac{p_g}{\Delta p_g} \\ \varepsilon_{gf}=\dfrac{\Delta Q_g}{Q_g}\cdot\dfrac{p_f}{\Delta p_f} & \varepsilon_{gp}=\dfrac{\Delta Q_g}{Q_g}\cdot\dfrac{p_p}{\Delta p_p} & \varepsilon_{gg}=\dfrac{\Delta Q_g}{Q_g}\cdot\dfrac{p_g}{\Delta p_g} \end{cases} \tag{5}$$

where, ε_{ff}, ε_{pp}, ε_{gg} - peak, level and valley self-elasticity coefficients.

ε_{fp}, ε_{fg}, ε_{pf}, ε_{pg}, ε_{gf}, ε_{gp} - cross-elasticity coefficient for any two time periods.

p_f, p_p, p_g - the price of electricity in peak, level and valley hours before the implementation of time-sharing tariffs.

Δp_f, Δp_p, Δp_g - the amount of price change in the peak, level and trough periods before the implementation of time-of-day tariffs.

Under the influence of time-sharing tariff, the relationship between the amount of electricity consumption and the amount of change in the price of electricity during the peak and valley periods is:

$$\begin{bmatrix} Q_{f'} \\ Q_{p'} \\ Q_{g'} \end{bmatrix}=\begin{bmatrix} Q_f \\ Q_p \\ Q_g \end{bmatrix}+\begin{bmatrix} Q_f & & \\ & Q_p & \\ & & Q_g \end{bmatrix}E\begin{bmatrix} \dfrac{\Delta p_f}{p_f} \\ \dfrac{\Delta p_p}{p_p} \\ \dfrac{\Delta p_g}{p_g} \end{bmatrix} \tag{6}$$

where, E - matrix of price elasticity of user demand.

The expression for the price elasticity of user demand matrix E is:

$$E=\begin{bmatrix} \varepsilon_{ff} & \varepsilon_{fp} & \varepsilon_{fg} \\ \varepsilon_{pf} & \varepsilon_{pp} & \varepsilon_{pg} \\ \varepsilon_{gf} & \varepsilon_{gp} & \varepsilon_{gg} \end{bmatrix} \tag{7}$$

Therefore, the time-sharing tariff is modeled as:

$$Q_{t'}=Q_t+\left[Q_t\left(\varepsilon_{tt}\cdot\frac{C'_{t'}-C_t}{C_t}+\varepsilon_{tt'}\cdot\frac{C'_{t'}-C_{t'}}{C_{t'}}\right)\right] \tag{8}$$

where $Q_{t'}$ - electricity consumption in Period t' after the implementation of time-of-use tariffs, Q_t - electricity consumption during t periods before the introduction of time-of-day tariffs, $C_{t'}$ - tariff for period t after the implementation of time-of-use tariffs, $C'_{t'}$ - After the introduction of time-of-use tariffs t' Time-of-use tariffs, C_t - Before the introduction of time-of-use tariffs t Time-of-use tariffs, $C_{t'}$ - Before the introduction of time-of-use tariffs t' Time-of-use tariffs.

III. A. 2) Incentivized Demand Response Modeling

Incentive Based Demand Response (IBDR) is a protocol designed by the power related authorities to incentivize customers to change their electricity consumption habits at some specific time periods, the main content of which can be roughly summarized as to cut down the customer loads during the peak periods of electricity consumption and to increase the customer loads during the trough periods of electricity consumption while satisfying the comfort level [21].

The cost function expression for IBDR is:

$$C_{IBDR}=\sum_{n=1}^{N}C_n\Delta L_n+\sum_{n=1}^{N}\sum_{m=1}^{M}E_{n,m}^{+}\Delta L_{n,m,t}^{+}+\sum_{n=1}^{N}\sum_{m=1}^{M}E_{n,m}^{-}\Delta L_{n,m,t}^{-} \tag{9}$$

where, C_{IBDR} - IBDR scheduling cost, C_n - IBDR unit response capacity cost, ΔL_n - User n response capacity, $\Delta L_{n,m,t}^{+}$, $\Delta L_{n,m,t}^{-}$ --Incremental and decremental capacity of user response to IBDR segment m at the moment of t, $E_{n,m}^{+}$, $E_{n,m}^{-}$ - Unit cost of power increase and unit cost of power decrease in segment m of the segmented function, N, M - The number of users participating in the IBDR and the number of segments in the multi-segment offer curve.

III. B. Optimizing the scheduling algorithm

III. B. 1) Optimizing Scheduling Objectives

In the dispatching cycle, the operating cost of the user's photovoltaic storage microgrid is taken as the optimization objective, and the microgrid operating cost function is constructed, which mainly considers the PV system power generation cost and battery operation cost, and the cost of power sales of the big grid, i.e., the subsidy cost of the big grid to supply power to the user's photovoltaic storage microgrid and the user's participation in demand response [22]. The total system cost objective function is:

$$\min C_{MG}(P)=\sum_{t=1}^{N}\left(C_{PV}P_{PV}^{t}+u_{BS}P_{BS}^{t}+f_{GD}P_{GD}^{t}+\lambda_{load}^{t}\right) \tag{10}$$

where, $C_{MG}(P)$ - total system operating cost (¥), C_{PV} - PV power generation cost coefficient (¥/kW), u_{BS} - battery power generation cost coefficient (¥/kW), f_{GD} - cost coefficient of purchasing and selling electricity in the big power grid (¥/kW), P_{PV}^{t} --Photovoltaic power output (¥/kW), P_{BS}^{t} - Battery storage system power generation (kW), P_{GD}^{t} - Power purchased and sold by the large power grid (kW), λ_{load}^{t} - Subsidized cost of user participation in demand response (¥).

(1) Solar photovoltaic power generation costs

Solar photovoltaic power generation belongs to the renewable energy power generation system. The power generation cost model is as follows:

$$\begin{cases} C_{RE}(P_i(t))=C_{RE.dep}(P_i(t))+C_{RE.om}(P_i(t))-C_{RE.sub}(P_i(t)) \\ C_{RE.dep}(P_i(t))=\sum_{i=1}^{N_{RE}}P_i(t)\left[\dfrac{r_i(1+r_i)^{n_i}}{(1+r_i)^{n_i}-1}\right]\left[\dfrac{c_{init.i}}{8760k_i}\right] \\ C_{RE.om}(P_i(t))=\sum_{i=1}^{N_{RE}}c_{RE.om}P_i(t) \\ C_{RE.sub}(P_i(t))=\sum_{i=1}^{N_{RE}}k_{RE}P_i(t) \end{cases} \tag{11}$$

where $C_{RE}(P_i(t))$ - solar photovoltaic power generation cost coefficient (¥ / kW), $C_{RE.dep}(P_i(t))$ - i rd solar photovoltaic power generation equipment output power depreciation costs (¥ / kW), $C_{RE.om}(P_i(t))$ - i th solar photovoltaic power plant output power operation and maintenance costs (¥ / kW), $C_{RE.sub}(P_i(t))$ - i th solar photovoltaic power generation equipment output power subsidy (¥ / kW), N_{RE} - Number of solar PV generator sets, r_i, n_i, $c_{init.i}$ - Discount rate, initial investment cost per unit capacity over the life cycle of the equipment, k, $c_{RE.om}$, k_{RE} - Annual utilization coefficient, operating cost coefficient of renewable energy generation and subsidy coefficient (¥/kW).

(2) Battery storage system operating costs

The operating cost of the energy storage battery system is mainly to calculate the power consumed in the process of discharging, and the corresponding results are obtained through the power generation cost coefficient. The battery storage system operating cost model is:

$$\begin{cases} \mu_{BS}(P_B(t)) = \gamma_{BS} \cdot P_{B.dch}(t) \\ \gamma_{BS} = \dfrac{C_{B.init}}{E_{B.a}} \end{cases} \tag{12}$$

where, $\mu_{BS}(P_B(t))$ - the generation cost of the battery storage system (¥/kW), $P_{B.dch}(t)$ - Power generation of battery energy storage system (kW), γ_{BS} --Generation cost coefficient of battery storage system (¥/kW), $C_{B.init}$ - Purchase cost of battery energy storage system (¥/kW), $E_{B.a}$ - Ratio, constant.

(3) Economic compensation cost

Economic compensation cost is due to scheduling the user's flexible load to participate in the supply and demand co-optimization, the need to give the user's compensation costs and the costs incurred. In this paper, the air conditioning load and washing machine load to participate in supply and demand co-optimization to take the form of economic compensation, the total economic compensation for:

$$\lambda_{load}^{t} = f_{AC} \cdot P_{AC}(t) + f_{WM} \cdot P_{WM}(t) \tag{13}$$

where, f_{AC} - unit economic compensation cost of air-conditioning load (¥/kW), $P_{AC}(t)$ - t moments of air-conditioning load reduction of the load (¥/kW), f_{WM} -- Unit economic compensation cost of washing machine load (¥/kW), $P_{WM}(t)$ - Load volume of washing machine load transfer at the moment of t (¥/kW).

III. B. 2) Constraints

Power balance is a very important indicator to realize the safe and reliable operation of microgrids, which means that the supply and demand power must be equal on the supply and demand sides [23].

(1) Photovoltaic power output constraint

The PV generation system operates in the maximum power tracking point mode, so the constraints are shown in equation (14):

$$P_{PV}^{\min}(t) \le P_{PV}(t) \le P_{PV}^{\max}(t) \tag{14}$$

where, $P_{PV}^{\min}(t)$, $P_{PV}^{\max}(t)$ - the minimum output power and maximum output power of the PV power generation system (kW).

(2) Battery storage system operation constraints

The constraints mainly include maximum charge capacity constraint and minimum charge capacity constraint, maximum charge/discharge constraint and minimum charge/discharge constraint, and the specific constraints are shown in equation (15):

$$\begin{cases} SOC_{BS}^{\min} \le SOC(t) \le SOC_{BS}^{\max} \\ P_{ch,BS}^{\min} \le P_{ch}^{BS}(t) \le P_{ch,BS}^{\max} \\ P_{dch,BS}^{\min} \le P_{dch}^{BS}(t) \le P_{dch,BS}^{\max} \end{cases} \tag{15}$$

where, $SOC_{BS}^{\min}$, $SOC_{BS}^{\max}$ - minimum charge state and maximum charge state of the battery storage system, $P_{ch,BS}^{\min}$, $P_{ch,BS}^{\max}$ - battery storage system minimum charging power and maximum charging power (kW), $P_{dch,BS}^{\min}$, $P_{dch,BS}^{\max}$ - battery storage system minimum discharge power and maximum discharge power (kW).

(3) Microgrid and large grid power interaction constraints

The microgrid operates grid-connected when there is a power shortage in the microgrid system or when the PV generation system generates sufficient power. When grid-connected, the two transfer energy is not without limitations, otherwise it will affect the system security, the constraint is shown in equation (16):

$$P_{GD}(t) \le P_{GD,\max} \tag{16}$$

where, $P_{GD}(t)$ - t moments microgrid and large grid interaction power (kW).

$P_{GD,\max}$ - Maximum interaction power between microgrid and large power grid (kW).

IV. Arithmetic simulation analysis

IV. A. Basic data

This paper samples central air conditioners and split air conditioners within an urban area, and in order to facilitate the calculation, 500 split air conditioners with rated power of 2.8kW and the same or similar parameters are selected for the split air conditioner load clustering to test the reasonableness of the proposed clustering method. It is assumed that the equivalent heat capacity C of the building to which the air conditioner belongs obeys N (0.20, 0.24) stochastic normal distribution, the equivalent thermal resistance R obeys N (5.62, 14) stochastic normal distribution, and the initial indoor temperature of the air conditioner users is uniformly distributed between [22, 29]°C. Considering the sensitivity of different types of air conditioner users to price, the air conditioner user groups can be divided into the following three types for discussion:

1) This type of air-conditioning users belong to the type that is not too sensitive to price and has high requirements for room temperature environment, so it is assumed that the permissible range of room temperature is [23, 25] °C.

2) This type of air-conditioning user belongs to the type of price sensitivity in general, the requirements of the room temperature environment is moderate, so it is assumed that the permissible range of room temperature is [23, 27] °C.

3) This type of air-conditioning users belongs to the type of price-sensitive, relatively low requirements for room temperature environment, so it is assumed that the permissible range of room temperature is [23, 29] °C.

IV. B. Efficiency of air conditioning load scheduling considering comfort level

Since the human comfort index and the room temperature allowable range are closely related, the number of hours and capacity of air-conditioning load clusters that can be involved in scheduling changes when the human comfort evaluation index is taken into account.

(1) For split AC load clusters, when the evaluation criterion is the TSV indicator, the allowable range of room temperature for the third category of users is narrowed from [23, 29] °C to [23, 27.6] °C, and the upper and lower ranges of room temperatures for the first and second categories of users are not affected. The updated allowable participation scheduling hours and allowable participation scheduling capacity for the three categories of air conditioning users are shown in Table 1:

Table 1: Time and capacity for scheduling

Air conditioning user category	Comfort type	General type	Economy budget
Room room range(°C)	[23,25]	[23,27]	[23,27.6]
Manageable length	5.3	12.9	13.8
Scheduling capacity (MW)	0.50	0.54	0.54

When the evaluation criterion is the THI indicator, the permissible range of room temperature for the third category of users is further reduced from [23, 29] °C to [23, 26.4] °C, the permissible range of room temperature for the second category of users is reduced from [23, 27] °C to [23, 26.4] °C, and the upper and lower ranges of room temperature for the first category of users are not affected. The updated allowable participating scheduling hours and allowable participating scheduling capacity for the three categories of air conditioning users are shown in Table 2.

Table 2: Time and capacity for scheduling

Air conditioning user category	Comfort type	General type	Economy budget
Room room range(°C)	[23,25]	[23,26.4]	[23,26.4]
Manageable length	5.3	8.8	9.2
Scheduling capacity (MW)	0.50	0.0	0.50

Comparing the results of the above two tables and the example analysis, it can be seen that when the split air conditioning load clusters take into account the human comfort index, the number of hours that can be involved in scheduling decreases compared to those that do not take into account the human comfort index, but the capacity that can be involved in scheduling does not change much due to the influence of the cluster size.

(2) For central air-conditioning load clusters, when the evaluation criterion is the TSV indicator, the allowable range of room temperature for the third category of users is narrowed from [23, 29] °C to [23, 28.2] °C, and the upper and lower ranges of room temperatures for the first and second categories of users are not affected. The updated allowable participation scheduling hours and allowable participation scheduling capacity for the three categories of air conditioning users are shown in Table 3.

Table 3: Time and capacity for scheduling

Air conditioning user category	Comfort type	General type	Economy budget
Room room range(°C)	[23,25]	[23,27]	[23,28.2]
Manageable length	7.56	17.4	21.8
Scheduling capacity (MW)	10.3	13.0	13.8

When the evaluation criterion is the THI indicator, the permissible range of room temperature for the third category of users is further reduced from [23, 29] °C to [23, 26.5] °C, the permissible range of room temperature for the second category of users is reduced from [23, 27] °C to [23, 26.7] °C, and the upper and lower ranges of room temperature for the first category of users are not affected. The updated allowable participating scheduling hours and allowable participating scheduling capacity for the three categories of air conditioning users are shown in Table 4.

Table 4: Time and capacity for scheduling

Air conditioning user category	Comfort type	General type	Economy budget
Room room range(°C)	[23,25]	[23,26.7]	[23,26.5]
Manageable length	7.38	12.0	11.7
Scheduling capacity (MW)	10.3	12.0	11.7

Comparison of the results of the tables and the analysis of the examples shows that when the central air conditioning load clusters take into account the human comfort index, the number of hours that can be involved in the scheduling is reduced and the capacity that can be involved in the scheduling is slightly reduced, compared to the case when the human comfort index is not taken into account.

IV. C. Real-time scheduling results

In this paper, energy storage is used as the scheduling object in the real-time scheduling phase, and the optimal scheduling is performed according to the proposed scheduling method. When the deviation coefficient is small, the basic time granularity (15min in this paper) is selected. When the deviation coefficient is large, a smaller time granularity is selected (5min, 3min in this paper). The 24-hour deviation coefficients are obtained based on the forecast data of the net load as well as the model as shown in Fig. 1. From the figure, it can be seen that there are two periods in 24 hours with large deviation coefficients, i.e., large fluctuations in net load, namely, 4:00-6:00 and 17:00-19:00, and according to the time granularity selection model, real-time scheduling is carried out for the period of 5:00-6:00 by taking 3min as the time granularity, and real-time scheduling is carried out for the period of 18:00-19:00 by using 5min as the time granularity, and real-time scheduling is kept at the base time granularity for the rest of the time. And the base time granularity of 15min is maintained for the rest of the hours.

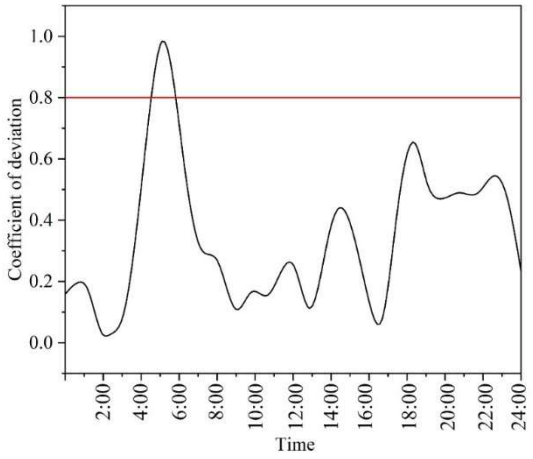

Figure 1: deviation diagram

Scheduled at time granularity of 3 min and base time granularity of 15 min, the power as well as storage response of the contact line is shown in Fig. 2, respectively.

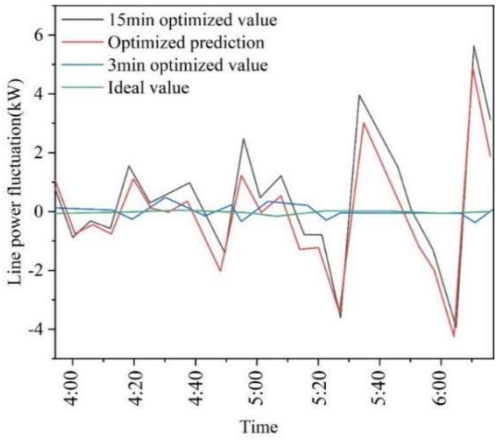

(a) The power of the contact line of 19:00 real-time scheduling

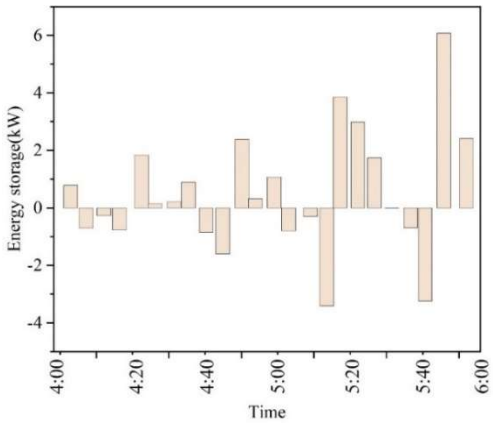

(b) 5min time particle energy storage response

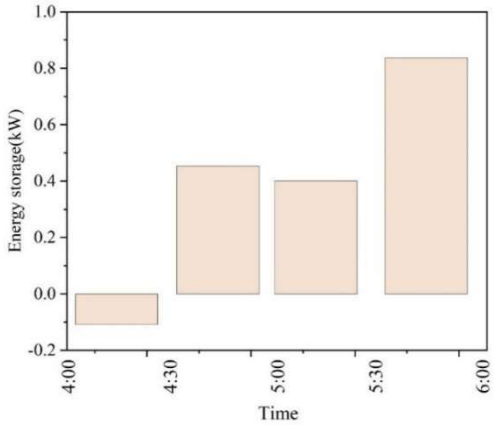

(c) 15min time particle energy storage response

Figure 2: Communication line power and energy storage response

Scheduled at time granularity of 5 min and base time granularity of 15 min, the power as well as storage response of the contact line is shown in Fig. 3, respectively.

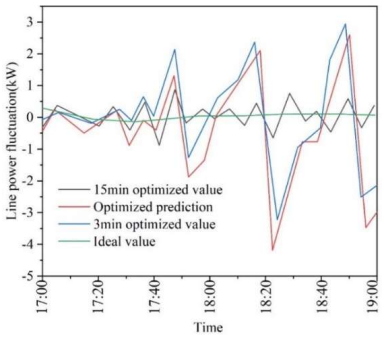

(a) The power of the contact line of 19:00 real-time scheduling

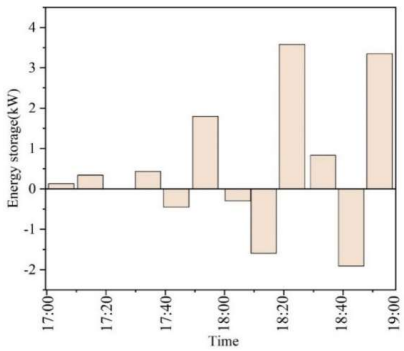

(b) 5min time particle energy storage response

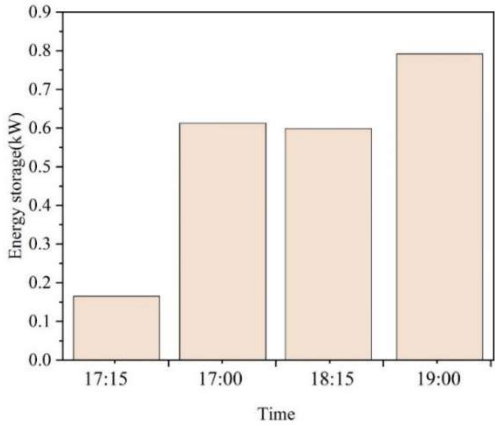

(c) 15min time particle energy storage response

Figure 3: Communication line power and energy storage response

From the above figure, it can be seen that compared with scheduling with a time granularity of 15 min, the contact line power obtained by real-time optimized scheduling with a time granularity of 3 min or 5 min is obviously closer to the ideal value obtained by scheduling a few days ago, and the purpose of suppressing the contact line power can be achieved. Moreover, real-time scheduling with a time granularity of 15 min has little effect on the optimization of real-time predicted contact line power in both time periods.

The results of the optimized scheduling with different time granularities under two time periods are shown in Table 5. The contact line power difference in the table is the absolute value of the difference between the optimized contact line power and the ideal contact line power, and the value is taken as the average value of the whole time period. From the table, it can be seen that although reducing the time granularity can reduce the contact line power difference and smooth out the contact line fluctuation. However, it will increase the real-time scheduling cost and computation, so it is necessary to choose different time granularity in different time periods to achieve a balance between the degree of fluctuation of the contact line and the scheduling cost and computation.

Table 5: different time particle optimization scheduling results

Time period	Time grain	Line power difference (KW)	Total running cost (yuan)	Iteration number
4:00-6:00	3min	0.25	150.03	335
	15min	1.63	274.96	56
17:00-19:00	3min	0.40	220.46	170
	15min	1.28	290.36	48

V. Conclusion

The data acquisition and optimal scheduling algorithm for air conditioning equipment oriented to grid supply and demand regulation effectively realizes the participation of air conditioning loads in grid supply and demand regulation under the premise of guaranteeing user comfort. The temperature prediction model established by the extreme learning machine can accurately predict the indoor temperature changes, and then evaluate the adjustable capacity of air-conditioning loads. The results show that, for the split air conditioning load clusters, when the TSV index is applied to evaluate human comfort, the allowable range of room temperature for general type users is 23-27°C, and the allowable time to participate in dispatch is up to 12.9 minutes, with a dispatchable capacity of 0.54 MW; for the comfort type users, the allowable range of room temperature is 23-25°C, and the allowable time to participate in dispatch is up to 5.3 minutes, with a dispatchable capacity of 0.50 MW. When the THI index is used, the allowable range of room temperature is reduced to 23-26.4°C for both general and economic users, and the scheduling capacity is somewhat limited. Through the time granularity optimization strategy, during the 4:00-6:00 high deviation coefficient time period, using 3-minute time granularity for real-time scheduling, the power difference of the contact line is only 0.25kW, with a total operating cost of 150.03 yuan, and the number of iterations is 335; and when 15-minute time granularity is used for the same time period, the power difference of the contact line

reaches 1.63kW, and the total operating cost increases to 274.96 dollars and the number of iterations is reduced to 56 times. This shows that the appropriate reduction of time granularity can effectively smooth the power fluctuation of the contact line, but will increase the amount of computation and the number of scheduling, and it is necessary to choose the appropriate time granularity in different time periods in order to achieve a balance between the degree of fluctuation of the contact line and the cost of scheduling and the amount of computation.

References

[1] Xu, X., Zhong, Z., Deng, S., & Zhang, X. (2018). A review on temperature and humidity control methods focusing on air-conditioning equipment and control algorithms applied in small-to-medium-sized buildings. Energy and buildings, 162, 163-176.

[2] Yousaf, S., Bradshaw, C. R., Kamalapurkar, R., & San, O. (2023). Investigating critical model input features for unitary air conditioning equipment. Energy and Buildings, 284, 112823.

[3] Kindaichi, S., Nishina, D., Murakawa, S., Ishida, M., & Ando, M. (2017). Analysis of energy consumption of room air conditioners: An approach using individual operation data from field measurements. Applied Thermal Engineering, 112, 7-14.

[4] Dong, B., Kjærgaard, M. B., De Simone, M., Gunay, H. B., O'Brien, W., Mora, D., ... & Zhao, J. (2018). Sensing and data acquisition. Exploring occupant behavior in buildings: Methods and Challenges, 77-105.

[5] Sarma, P., Singh, H. K., & Bezboruah, T. (2018). A real-time data acquisition system for monitoring sensor data. Int. J. Comput. Sci. Eng, 6(6), 539-542.

[6] Lim, J. S. (2019). A design of small size sensor data acquisition and transmission system. Journal of Convergence for Information Technology, 9(1), 136-141.

[7] Balakrishna, S., Thirumaran, M., & Solanki, V. K. (2018). A framework for IoT sensor data acquisition and analysis. EAI Endorsed Transactions on Internet of Things, 4(16), e4-e4.

[8] Mobaraki, B., Komarizadehasl, S., Castilla Pascual, F. J., Lozano-Galant, J. A., & Porras Soriano, R. (2022). A novel data acquisition system for obtaining thermal parameters of building envelopes. Buildings, 12(5), 670.

[9] Miqdad, A., Kadir, K., & Ahmed, S. F. (2017, November). Development of data acquisition system for temperature and humidity monitoring scheme. In 2017 IEEE 4th International Conference on Smart Instrumentation, Measurement and Application (ICSIMA) (pp. 1-4). IEEE.

[10] Huang, C. (2021, December). Design of Central Air Conditioning Control Acquisition Device Based on IoT Technology. In Journal of Physics: Conference Series (Vol. 2143, No. 1, p. 012002). IOP Publishing.

[11] Wang, W., Zhang, Z., Cui, H., Cui, J., & Gao, C. (2025). Design of real-time data acquisition and regulation algorithm of air-conditioning equipment for grid supply-demand interaction. J. COMBIN. MATH. COMBIN. COMPUT, 127, 6885-6906.

[12] Castro, A., Martínez-Osuna, J. F., Michel, R., Escoto-Rodríguez, M., Bullock, S. H., Cueva, A., ... & Vargas, R. (2017). A low-cost modular data-acquisition system for monitoring biometeorological variables. Computers and Electronics in Agriculture, 141, 357-371.

[13] Chua, K. J., Chou, S. K., Yang, W. M., & Yan, J. (2013). Achieving better energy-efficient air conditioning–a review of technologies and strategies. Applied energy, 104, 87-104.

[14] Yang, S., Yu, J., Gao, Z., & Zhao, A. (2023). Energy-saving optimization of air-conditioning water system based on data-driven and improved parallel artificial immune system algorithm. Energy Conversion and Management, 283, 116902.

[15] Lee, D., & Tsai, F. P. (2020). Air conditioning energy saving from cloud-based artificial intelligence: Case study of a split-type air conditioner. Energies, 13(8), 2001.

[16] Chen, W. H., Mo, H. E., & Teng, T. P. (2018). Performance improvement of a split air conditioner by using an energy saving device. Energy and Buildings, 174, 380-387.

[17] Karali, N., Shah, N., Park, W. Y., Khanna, N., Ding, C., Lin, J., & Zhou, N. (2020). Improving the energy efficiency of room air conditioners in China: Costs and benefits. Applied Energy, 258, 114023.

[18] Lee, D., & Tsai, F. P. (2020). Air conditioning energy saving from cloud-based artificial intelligence: Case study of a split-type air conditioner. Energies, 13(8), 2001.

[19] Yao, L., & Huang, J. H. (2019). Multi-objective optimization of energy saving control for air conditioning system in data center. Energies, 12(8), 1474.

[20] Sujan Ghimire,Ravinesh C. Deo,Konstantin Hopf,Hangyue Liu,David Casillas Pérez,Andreas Helwig... & Sancho Salcedo Sanz. (2025). Half-hourly electricity price prediction model with explainable-decomposition hybrid deep learning approach. Energy and AI,20,100492-100492.

[21] Tung TrieuDuc,Anh NguyenTuan,Tuyen NguyenDuc & HirotakaTakano. (2024). Energy management of hybrid AC/DC microgrid considering incentive‐based demand response program. IET Generation, Transmission & Distribution,18(21),3289-3302.

[22] Gang Liu,Enhui Jiang,Donglin Li,Jieyu Li,Yuanjian Wang,Wanjie Zhao & Zhou Yang. (2025). Annual multi-objective optimization model and strategy for scheduling cascade reservoirs on the Yellow River mainstream. Journal of Hydrology,659,133306-133306.

[23] Joseph R. Farah,D. Andrew Howell,Giacomo Terreran,Ido Irani,Jonathan Morag,Craig Pellegrino... & Daichi Hiramatsu. (2025). Shock-cooling Constraints via Early-time Observations of the Type IIb SN 2022hnt. The Astrophysical Journal,984(1),60-60.